

Conformal windows of $SP(2N)$ and $SO(N)$ gauge theories from topological excitations on $\mathbb{R}^3 \times S^1$

Siavash Golkar

Department of Physics, University of Toronto, Toronto, ON M5S-1A7, Canada

*E-mail: sgolkar@physics.utoronto.ca **

ABSTRACT: We derive an estimate of the lower boundary of the conformal window of $SP(2N)$ and $SO(N)$ gauge theories with fermionic matter in several different representations. We calculate the index of topological excitations for these groups on the manifold $\mathbb{R}^3 \times S^1$, from which we deduce the scale of the generation of the mass gap of the theory. This is then used to approximate the critical value of the number of species n_f^* for the onset of conformality on \mathbb{R}^4 . We also provide a detailed comparison with other estimates of the conformal window.

*Changing to golkar@u.washington.edu as of October 1st 2009.

Contents

1. Introduction	1
1.1 Motivation	1
1.2 Outline	2
1.3 Notation	2
2. The Index of the Dirac operator	3
2.1 Monopole Backgrounds	3
2.2 Calculating the index	5
3. Conformality bounds	8
3.1 Conformal windows for $SP(2N)$	8
3.1.1 $SP(2N)$ with n_f fundamental fermions	10
3.1.2 $SP(2N)$ with adjoint fermions	11
3.1.3 $SP(2N)$ with 2-index anti-symmetric fermions	11
3.2 Conformal windows for $SO(2N + 1)$	12
3.2.1 $SO(2N + 1)$ with fundamental fermions	13
3.2.2 $SO(2N + 1)$ with adjoint fermions	13
3.2.3 $SO(2N + 1)$ with 2-index symmetric fermions	14
3.3 Conformal windows for $SO(2N)$	14
3.3.1 $SO(2N)$ with fundamental fermions	15
3.3.2 $SO(2N)$ with adjoint fermions	15
3.3.3 $SO(2N)$ with 2-index symmetric fermions	16
4. Comparison with other estimates of the conformal window	16
5. Conclusion	18
A. Lie Algebra Preliminaries	19

1. Introduction

1.1 Motivation

In recent years, theories with strong gauge dynamics at or near conformality, specifically those in four dimensions, have been receiving an increasing amount of attention. One of the most pertinent areas of their applicability is arguably the problem of electroweak symmetry breaking. It is conceivable that the breaking of electroweak symmetry might be induced by a strongly coupled gauge theory without Higgs scalars. It is well known that utilizing

an appropriately rescaled QCD cannot explain electroweak precision data, however, it has been argued that gauge sectors with near-conformal or conformal behavior can help solve phenomenological problems of fine-tuning and flavor in models of dynamical electroweak symmetry breaking [1, 2, 3, 4]. The more recent formalism of “unparticle physics” is also heavily dependent on conformal theories [5].

However, the very nature of these strongly coupled gauge theories makes them difficult subjects of study to the point that there is currently no definitive method of determining which asymptotically free gauge theories flow to conformal field theories in the infrared. Given the relevance of these theories in different areas of high energy physics, the exploration of the parameter space is surely warranted.

1.2 Outline

The general idea behind our calculation is given in section 3. The reader primarily interested in our final results can skip over to section 4 where our results have been summarized in tables 4.1 through 4.6. In the rest of the paper we provide a more detailed calculation of the conformal window of several classes of gauge theories.

We begin in chapter 2, where we calculate the index of topological excitation on $\mathbb{R}^3 \times S^1$ by generalizing the results of [6]. In section 2.1 we introduce the backgrounds of interest which are comprised of Prasad-Sommerfield solutions of $SU(2)$ embedded into a general gauge group G as well as the four dimensional instanton and their combinations. In 2.2 we explicitly derive the index of these objects and demonstrate that for small circle sizes, unsurprisingly, it is equal to the Callias index [7].

Section 3 is the heart of our discussion. After a brief overview of the methodology, we provide detailed calculations of the mass gap as well as the conformal windows of several different representations of $SP(2N)$, $SO(2N+1)$ and $SO(2N)$ gauge groups, respectively in sections 3.1, 3.2 and 3.3. These results are summarized in tables 4.1 through 4.6 in section 4, where we also provide detailed comparisons with the results of two other approaches: the ladder approximation using truncated Schwinger-Dyson equations and the NSVZ-inspired approach with both $\gamma = 1$ and $\gamma = 2$.

In section 5 we conclude, discuss the shortcomings of our approach and provide possible directions for future work. Section 1.3 provides explains our notation and section A summarizes a few facts about Lie algebras we use throughout the paper.

1.3 Notation

We work with the four dimensional Euclidean Dirac operator in representation R :

$$\not{D} = \gamma_\mu D_\mu \quad , \quad D_\mu = \partial_\mu + iA_\mu^a T^a, \quad (1.1)$$

where the matrices T^a (along with other Lie algebra related notations) are defined in appendix A. Throughout the paper, Roman indices from the beginning of the alphabet are Lie algebra indices, Roman indices from the middle of the alphabet run from 1 to 3 and correspond to the non-compactified coordinates, Greek indices from the beginning of the alphabet refer to roots of the Lie algebra and Greek indices from the middle of the

alphabet run from 1 to 4 and correspond to the four dimensional manifold. We also take $x^4 \equiv y$ to be the direction along the compactified dimension with $y \sim y + L$.

Our choice of the gamma matrices is:

$$\gamma_k = \sigma_1 \otimes \sigma_k, \quad \gamma_4 = -\sigma_2 \otimes \mathbb{1}, \quad \gamma_5 = \sigma_3 \otimes \mathbb{1}, \quad (1.2)$$

where σ_k are the Pauli matrices. The vector-like Dirac operator is then:

$$\mathcal{D} = \begin{pmatrix} 0 & \sigma_k D_k + i\sigma_0 D_4 \\ \sigma_k D_k - i\sigma_0 D_4 & 0 \end{pmatrix} \equiv \begin{pmatrix} 0 & -D^\dagger \\ D & 0 \end{pmatrix}, \quad (1.3)$$

where we have defined the Weyl operator D . We have:

$$DD^\dagger = -D_\mu D^\mu + \sigma_m \frac{1}{2} \epsilon_{mkl} F_{kl} - \sigma_k F_{4k} = -D_\mu D^\mu, \quad (1.4a)$$

$$D^\dagger D = -D_\mu D^\mu + \sigma_m \frac{1}{2} \epsilon_{mkl} F_{kl} + \sigma_k F_{4k} = -D_\mu D^\mu + 2\sigma^m B^m, \quad (1.4b)$$

where D_μ is as in (1.1) and we have assumed, without loss of generality, that the background is anti-self-dual, i.e. $F_{4k} = \frac{1}{2} \epsilon_{klm} F_{lm} = B_k$.

2. The Index of the Dirac operator

In this section we rewrite the results of [6] for general gauge groups¹. Following their notation we let $U(x)$ be the holonomy of the Wilson line wrapping around the compact direction:

$$U = P \exp i \oint A_4 dy, \quad x \in \mathbb{R}^3, y \in S^1, \quad (2.1)$$

where A_4 is the component of the gauge field along the circle. In the weak coupling regime, A_4 behaves as a compact adjoint Higgs field and its asymptotic value $A_4|_\infty$ induces gauge symmetry breaking. Here, we assume that the symmetry breaking is maximal or equivalently $\alpha(A_4|_\infty) \neq 0, \forall \alpha \in \Phi$. This allows us to choose a base Δ , with respect to which A_4 is strictly dominant.

2.1 Monopole Backgrounds

There are two classes of nontrivial topological excitations on $\mathbb{R}^3 \times S^1$ [9, 10]. The first is the generalization of the three-dimensional $SU(2)$ Prasad-Sommerfield monopole and is y -independent. For a gauge group G of rank l , there are l independent such solutions obtained by embeddings of the $SU(2)$ solution in G . We construct them as follows.

Let $\varphi^s(x, \lambda)$ and $A_j^s(x, \lambda)$ be the $SU(2)$ monopole solution corresponding to a vacuum expectation value λ . In regular (hedgehog) gauge we have:

$$\begin{aligned} \varphi^s(x, \lambda) &= \frac{\hat{x}^s}{|x|} (1 - \lambda|x| \coth \lambda|x|), \\ A_j^s(x, \lambda) &= \epsilon_{sjk} \hat{x}^k \left(\frac{1}{|x|} - \frac{\lambda}{\sinh \lambda|x|} \right). \end{aligned} \quad (2.2)$$

¹These results can be derived directly from [8].

Let α be any root and take:

$$\begin{aligned} t_\alpha^1 &= \frac{1}{2}(x_\alpha + y_\alpha), \\ t_\alpha^2 &= \frac{i}{2}(y_\alpha - x_\alpha), \\ t_\alpha^3 &= \frac{1}{2}h_\alpha, \end{aligned} \tag{2.3}$$

with x_α , y_α and h_α as in appendix A. Then,

$$\begin{aligned} A_4(x) &= \sum_{s=1}^3 \varphi^s(x, \lambda) t_\alpha^s + A_4|_\infty - \alpha(A_4|_\infty) t_\alpha^3, \\ A_j(x) &= \sum_{s=1}^3 A_j^s(x, \lambda) t_\alpha^s, \end{aligned} \tag{2.4}$$

with $\lambda = -\alpha(A_4|_\infty)$, is an elementary anti-self-dual monopole solution corresponding to the root α , satisfying $F_{4k} = -\frac{1}{2}\epsilon_{4kpq}F_{pq} = \frac{1}{2}\epsilon_{kpq}F_{pq} = B_k$ [11]. The asymptotic behavior of this solution in the string gauge is given as:

$$\begin{aligned} A_4 &\rightarrow A_4|_\infty - \frac{1}{|x|} t_\alpha^3, \\ B_j &\rightarrow \frac{\hat{x}^j}{|x|^2} t_\alpha^3, \end{aligned} \tag{2.5}$$

which gives magnetic charge $-\alpha^*$ and topological charge $\frac{L}{2\pi}\alpha^*(A_4|_\infty)$. The independent monopoles are the solutions corresponding to the l simple roots.

The second class is comprised of solutions that wrap around the compact dimension [9, 10], most of these can be obtained from the first class solutions via non-periodic gauge transformations. We start with the solution (2.4) corresponding to a root α and we apply the gauge transformation:

$$U_\alpha(y) = \exp\left(\frac{i2\pi}{L} y t_\alpha^3\right). \tag{2.6}$$

However, the asymptotic value of this solution is shifted by:

$$A'_4(x, y)|_{|x|\rightarrow\infty} = A_4|_\infty - \frac{2\pi}{L} t_\alpha^3. \tag{2.7}$$

To compensate for this shift, we use the solution (2.4) with a vacuum expectation $A_4|_\infty$ shifted in the other direction. The new solution is then given by:

$$\begin{aligned} A_4(x) &= \sum_{s=1}^3 \varphi^s(x, \lambda) t'^s + A_4|_\infty - \alpha(A_4|_\infty) t_\alpha^3 - \frac{2\pi}{L} t_\alpha^3, \\ A_j(x) &= \sum_{s=1}^3 A_j^s(x, \lambda) t'^s, \end{aligned} \tag{2.8}$$

with $\lambda = -\alpha(A_4|_\infty + \frac{2\pi}{L} t_\alpha^3)$ and t'^s defined as:

$$t'^s = U_\alpha t_\alpha^s U_\alpha^{-1}. \tag{2.9}$$

These transformations do not change the magnetic charge of the solution but decrease the topological charge by 1. One can therefore consider this new solution as a monopole corresponding to the root α combined with an (anti)-instanton of charge -1. In the same way, one can construct towers of solutions on top of the l basic solutions (2.4) by consecutively applying the gauge transformation (2.6) while compensating the vacuum shift in a similar manner to the solution obtained above.

However, there exists an independent tower of solutions built on top of the lowest root $\tilde{\alpha}$, defined in (A.8). Note that although these solutions correspond to a negative root, they are not anti-monopoles which would satisfy self-dual equations (Remember we defined our monopoles to satisfy anti-self-dual equations.) [9, 10, 12]. We construct them as follows. Start with the solution (2.4) for $\alpha = -\tilde{\alpha}$.

First, we define a new solution with an asymptotic value $A'_4|_\infty = \sigma_\alpha(A_4|_\infty) + n\pi h_\alpha$, where σ_α is the Weyl reflection² in α . Then we perform a Weyl reflection and the gauge transformation (2.6) to restore the asymptotic value of A_4 . The final solution is:

$$\begin{aligned} A_4(x) &= \sum_{s=1}^3 \varphi^s(x, \lambda) t'^s + A_4|_\infty + \alpha(A_4|_\infty) t_\alpha^3 - \frac{\pi}{L} h_\alpha, \\ A_j(x) &= \sum_{s=1}^3 A_j^s(x, \lambda) t'^s, \end{aligned} \tag{2.11}$$

with $\lambda = -\alpha(A'_4|_\infty)$ and t'^s defined as:

$$t'^s = U_\alpha \sigma_\alpha(t_\alpha^s) U_\alpha^{-1}. \tag{2.12}$$

The magnetic charge of this solution is $-\tilde{\alpha}^*$ and the topological charge is $\frac{L}{2\pi} \tilde{\alpha}^*(A_4|_\infty) - 1$.

2.2 Calculating the index

Now, we calculate the number of zero modes associated with the excitations discussed above. We follow the procedure of [6]. The Callias index of a Weyl fermion for a representation R is defined as:

$$I_R = \lim_{M^2 \rightarrow 0} \text{Tr} \frac{M^2}{D^\dagger D + M^2} - \text{Tr} \frac{M^2}{D D^\dagger + M^2}. \tag{2.13}$$

This function counts the difference of the number of zero modes of the operator D and the operator D^\dagger . We rewrite this as:

$$I_R(M^2) = \text{Tr} \gamma_5 \frac{M^2}{-\mathcal{B}^2 + M^2} = M \text{Tr} \gamma_5 \frac{\mathcal{B} + M}{-\mathcal{B}^2 + M^2} = -M \text{Tr} \gamma_5 \frac{1}{\mathcal{B} - M}, \tag{2.14}$$

²We use the correspondence between the elements of the Cartan and the weights explained in appendix A to define $\sigma_\alpha(A_4|_\infty)$. If w is the weight corresponding to $A_4|_\infty$ then

$$\sigma_\alpha(A_4|_\infty) = t_{\sigma_\alpha(w)}. \tag{2.10}$$

where in the second equality holds because of the cyclicity of the trace. We note that the expression in the trace is just the propagator of a fermionic field with action $S = \bar{\psi}(\not{D} - M)\psi$. For such theories in a locally four dimensional background we have:

$$\partial_\mu J_\mu^5 = \partial_\mu (\bar{\psi}\gamma_\mu\gamma_5\psi) = -2M\bar{\psi}\gamma_5\psi - \frac{1}{8\pi^2}T(R)\epsilon_{\mu\nu\rho\sigma}G_{\mu\nu}^a G_{\rho\sigma}^a, \quad (2.15)$$

where the first term is the explicit axial symmetry breaking and the second term is the topological contribution to the axial current. Using this identity we rewrite (2.14) as:

$$\begin{aligned} I_R(M^2) &= -M\text{Tr}\gamma_5 \langle \psi\bar{\psi} \rangle = M \int d^3x \int_0^L dy \langle \bar{\psi}\gamma_5\psi \rangle, \\ &= -\frac{1}{2} \int_{S_\infty^2} d^2\sigma^k \int_0^L dy \langle J_k^5 \rangle - \frac{T(R)}{16\pi^2} \int d^3x \int_0^L dy \epsilon_{\mu\nu\rho\sigma} G_{\mu\nu}^a G_{\rho\sigma}^a, \end{aligned} \quad (2.16)$$

where in the third equality the surface integral of $\partial_y \langle J_4^5 \rangle$ over the compact direction vanishes. Having separated the contribution of the topological charge, we now revert the first term to a form similar to (2.13) by doing the manipulations that took us from (2.13) to (2.14) in the other direction. Using the explicit form of the operators from (1.3) and (1.4), we get:

$$\begin{aligned} I_R^1(M^2) &\equiv -\frac{1}{2} \int_{S_\infty^2} d^2\sigma^k \int_0^L dy \langle J_k^5 \rangle = -\frac{1}{2} \int_{S_\infty^2} d^2\sigma^k \int_0^L dy \langle x | \gamma^k \gamma_5 \not{D} \frac{1}{-\not{D}^2 + M^2} | x \rangle \\ &= \frac{1}{2} \int_{S_\infty^2} d^2\sigma^k \int_0^L dy \text{tr} \langle x | \sigma^k \sigma^l D_l \left(\frac{1}{-D_\nu^2 + M^2 + 2\sigma^m B^m} - \frac{1}{-D_\nu^2 + M^2} \right) | x \rangle \\ &\quad - \frac{1}{2} \int_{S_\infty^2} d^2\sigma^k \int_0^L dy \text{tr} \langle x | i\sigma^k D_4 \left(\frac{1}{-D_\nu^2 + M^2 + 2\sigma^m B^m} + \frac{1}{-D_\nu^2 + M^2} \right) | x \rangle. \end{aligned} \quad (2.17)$$

This brings us to the final form of the index formula which will be used for the calculation:

$$I_R(M^2) = I_R^1(M^2) - 2T(R)Q, \quad (2.18)$$

where I_R^1 is defined above and $Q = \frac{1}{32\pi^2} \int d^3x \int_0^L dy \epsilon_{\mu\nu\rho\sigma} G_{\mu\nu}^a G_{\rho\sigma}^a$ is the topological charge, the values of which are given in section 2.1.

We now compute the contribution of the surface term I_R^1 for a composite monopole made up of n_α fundamental monopoles of type α , where $\alpha \in \tilde{\Delta}$.

The integrals in (2.17) are evaluated at infinity in \mathbb{R}^3 where we have:

$$-D_\nu^2 + M^2 \approx -\partial_m^2 + M^2 - D_4^2, \quad \text{with} \quad -iD_4 \rightarrow \frac{2\pi n}{L} + A_4. \quad (2.19)$$

Using this and (2.5), we expand (2.17) in B^k . The first term contribution vanishes after taking the Pauli matrix trace and we have:

$$\begin{aligned}
I_R^1(M^2) &= 2 \int_0^L dy \int_{S_\infty^2} d^2\sigma^k \text{tr} \langle x, y | iD_4 \frac{1}{-\partial_m^2 + M^2 - D_4^2} B^k \frac{1}{-\partial_m^2 + M^2 - D_4^2} |x, y\rangle, \\
&= -2 \int_0^L dy \int_{S_\infty^2} d^2\sigma^k \text{tr} \langle x, y | \left(\frac{2\pi n}{L} + A_4 \right)^2 \frac{1}{[-\partial_m^2 + M^2 + (\frac{2\pi n}{L} + A_4)^2]^2} \frac{\hat{x}^k}{|x|^2} t_\alpha^3 |x, y\rangle.
\end{aligned} \tag{2.20}$$

Evaluating these integrals ($d^2\sigma^k = |x|^2 x^k d\Omega_{S^2}$) at the $M \rightarrow 0$ limit, the surface contribution to the index of this excitation is:

$$I_R^1(0) = - \sum_{\alpha \in \tilde{\Delta}} \sum_{n \in \mathbb{Z}} n_\alpha \text{Tr}_R \left[\text{sign} \left(\frac{2\pi n}{L} + A_4 |_\infty \right) t_\alpha^3 \right]. \tag{2.21}$$

This sum is divergent. We regulate it following [6]:

$$\sum_{n=-\infty}^{\infty} \text{sign}(x+n) \rightarrow 1 - 2(x - \lfloor x \rfloor), \tag{2.22}$$

where $\lfloor x \rfloor = \text{Max} \{n \in \mathbb{Z} | n \leq x\}$ is the floor function. We have:

$$\begin{aligned}
I_R^1(0) &= 2 \sum_{\alpha \in \tilde{\Delta}} n_\alpha \text{Tr}_R \left[\left(\frac{L}{2\pi} A_4 |_\infty - \left\lfloor \frac{L}{2\pi} A_4 |_\infty \right\rfloor \right) t_\alpha^3 \right] \\
&= T(R) \sum_{\alpha \in \tilde{\Delta}} n_\alpha \alpha^* \left(\frac{L}{2\pi} A_4 |_\infty \right) - 2 \sum_{\alpha \in \tilde{\Delta}} n_\alpha \text{Tr}_R \left[\left\lfloor \frac{L}{2\pi} A_4 |_\infty \right\rfloor t_\alpha^3 \right],
\end{aligned} \tag{2.23}$$

where we have used the tracelessness of h_α . Plugging this into (2.18) and using the values of the topological charge from section 2.1 we have:

$$\begin{aligned}
I_R &= T(R) \sum_{\alpha \in \tilde{\Delta}} n_\alpha \alpha^* \left(\frac{L}{2\pi} A_4 |_\infty \right) - 2 \sum_{\alpha \in \tilde{\Delta}} n_\alpha \text{Tr}_R \left[\left\lfloor \frac{L}{2\pi} A_4 |_\infty \right\rfloor t_\alpha^3 \right] \\
&\quad - 2T(R) \sum_{\alpha \in \tilde{\Delta}} n_\alpha \alpha^* \left(\frac{L}{2\pi} A_4 |_\infty \right) + 2n_{\tilde{\alpha}} T(R) \\
&= 2T(R)n_{\tilde{\alpha}} - 2 \sum_{\alpha \in \tilde{\Delta}} n_\alpha \text{Tr}_R \left[\left\lfloor \frac{L}{2\pi} A_4 |_\infty \right\rfloor t_\alpha^3 \right].
\end{aligned} \tag{2.24}$$

We see that the non-integer contributions cancel and the final result is an integer.

From equation (2.24) we can see that if we take the n_α such that $\tilde{n} = 1$ and $\tilde{\alpha}^* + \sum n_\alpha \alpha^* = 0$, then the composite object would have zero magnetic charge, topological charge equal to -1 and index equal to $2T(R)$. These are the quantum numbers of the four dimensional (anti-)instanton. We can therefore conclude that the \mathbb{R}^4 instanton is made up

of monopoles with multiplicities given by the coefficients n_α , called the Kac labels, given in table A.1. This also shows that for the semi-classical expansion, composite objects made up of a few monopoles are more relevant than instantons.

For future reference, we also calculate the index in the small L limit, where equation (2.24) reduces to:

$$I_R = 2T(R)n_{\tilde{\alpha}} - \sum_{\alpha \in \tilde{\Delta}} n_\alpha \text{Tr}_R \left[\text{sign} \left(\frac{L}{2\pi} A_4|_\infty \right) t_\alpha^3 \right], \quad (2.25)$$

which is nothing but the Callias index on \mathbb{R}^3 [7].

3. Conformality bounds

In this section we calculate approximate bounds for the onset of conformality for QCD-like theories with general gauge groups. We follow the procedures developed in [13], which we summarize here.

The main idea behind our analysis is that, with a few assumptions, some properties of gauge theories with fermionic matter content in four dimensions can be inferred from their behavior on $\mathbb{R}^3 \times S^1$. In particular, the presence of a mass gap in the decompactification limit can be deduced from the L dependence of the mass gap m_σ at finite L . If we can assume that the behavior of m_σ as a function of L is persistent for all circle sizes then m_σ would only flow down to zero (and hence give us a conformal theory) if and only if it is a decreasing function with increasing L . Hence, the possibility of calculating m_σ in the regime $L \rightarrow 0$ gives us a criterion for conformality. In short, the theory in the decompactification limit is conformal (confining) if the mass gap is a decreasing (increasing) function of the circle size. As we will see, for small number of species n_f , m_σ is an increasing function of L and as n_f is increased beyond some value n_f^* the behavior flips. This critical number of species is then our estimate for the lower bound of the conformal window.

However, since the above assumption does not always hold, our prediction will be either an upper or a lower bound on the lower limit of the conformal window. The possibilities are classified in figure 3.1. If the mass gap of a theory behaves as in case C for some values of n_f , the mass gap is a decreasing function of L in the semi-classical regime, therefore, according to the conjecture above, the theory in the decompactification limit should be conformal. Of course this is incorrect because the mass gap asymptotes to a nonzero value. Hence, in this case the lower boundary of the conformal window is underestimated. A similar argument shows that in the case D, our procedure is an overestimate. For more details on peculiarities in the behavior of the mass gap, we refer the reader to [13].

3.1 Conformal windows for $SP(2N)$

The classic Lie group C_N or $SP(2N)$ has rank N , with $N - 1$ short roots and one long root. The extended Dynkin diagram is given in 3.2.

The vacuum is given by maximally separating the eigenvalues of the holonomy. We note that for the fundamental we would need to add a slight deformation to the effective

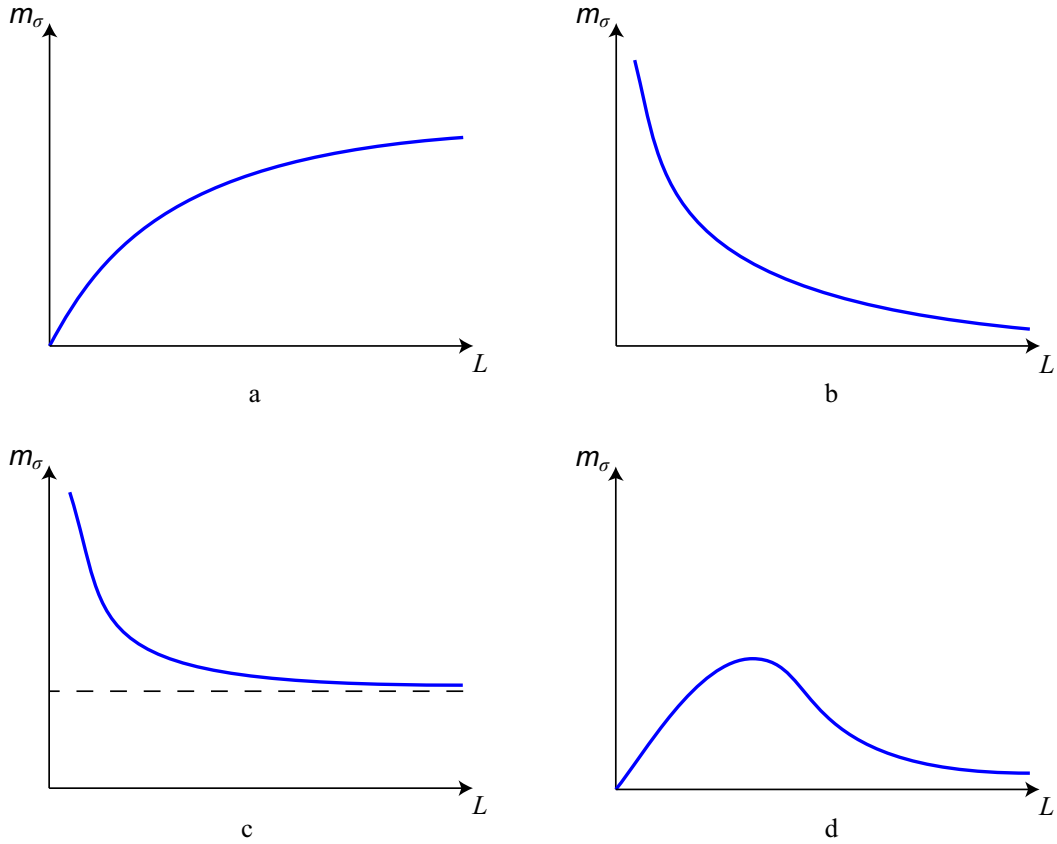


Figure 3.1: Possible behaviors of the mass gap of gauge fluctuations as a function of the size of the compactified direction. a) Mass gap increasing monotonically and approaching the R^4 value asymptotically. b) Mass gap is a monotonically decreasing function of L approaching zero in the decompactification limit. c) Mass gap is a monotonically decreasing function of L but approaches a non-zero asymptote in the decompactification limit. d) Mass gap is an increasing function of L in the semi-classical regime but the behavior flips and approaches zero at large L .

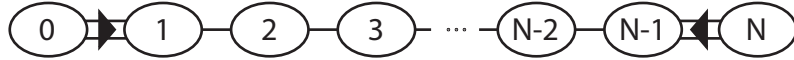


Figure 3.2: Extended Dynkin diagram of C_N . The extended root $\tilde{\alpha} = \alpha_0$ is proportional to λ_1 .

potential in order to achieve this structure (as in [14]) . The same holds for the 2-index anti-symmetric representation when $n_f = 1$. We have:

$$A_4|_{\infty} = \text{diag} \left(\frac{(2N-1)\pi}{2N}, \frac{(2N-3)\pi}{2N}, \dots, \frac{\pi}{2N}, -\frac{\pi}{2N}, -\dots, \frac{(2N-3)\pi}{2N}, -\frac{(2N-1)\pi}{2N} \right). \quad (3.1)$$

Since the monopole solutions corresponding to the simple roots are (anti-)self-dual, their

action is proportional to Q , their topological charge, via:

$$S_i = \frac{8\pi^2}{g^2} |Q_i|, \quad (3.2)$$

We also know that a composite object built up of monopoles with multiplicity κ_α is equivalent to the $4D$ instanton (see discussion under equation (2.24)). From this we deduce that the action of the monopole associated to the extended root $\tilde{\alpha}$ is:

$$\tilde{S} = \frac{8\pi^2}{g^2} - \sum_{\alpha \in \Delta} \kappa_\alpha S_\alpha, \quad (3.3)$$

where the first term is the action of the instanton. This gives $S_{\text{short}} = \frac{8\pi^2}{g^2 N}$ for the action of the fundamental monopoles corresponding to the short simple roots, α_i $1 \leq i \leq N-1$, and $S_{\text{long}} = \frac{4\pi^2}{g^2 N}$ for the long simple root α_N and $\tilde{\alpha}$. Now, if we had no matter content in our theory, the monopoles would be a source of mass for the dual photons, however, in the presence of fermions, the monopole operators get insertions of fermion fields attached to them:

$$\begin{aligned} M_j &= e^{-S_{\text{short}}} e^{2i\alpha_j \cdot \sigma} \psi^{I_j} & 1 \leq j \leq N-1 & \quad \text{short simple roots,} \\ M_j &= e^{-S_{\text{long}}} e^{i\alpha_j \cdot \sigma} \psi^{I_j} & j = 0, N & \quad \text{long simple root and } \tilde{\alpha}, \end{aligned} \quad (3.4)$$

where I_j is the index of the monopole associated to α_j , calculated in the $L \rightarrow 0$ limit from equation (2.25). Therefore, unless I_j is zero, the monopole operator M_j cannot generate mass for the dual photon combination $\alpha_j \cdot \sigma$, and we must look to higher order operators. We will further elaborate on this point in the examples below.

3.1.1 $SP(2N)$ with n_f fundamental fermions

In this case³, the only monopole with zero modes is the one associated to the long simple root α_N , which carries all the n_f zero modes of the instanton:

$$[I_0, I_1, \dots, I_{N-1}, I_N] = [0, 0, \dots, 0, 1]. \quad (3.5)$$

Therefore, the mass gap is generated through the $N-1$ monopole operators at order $e^{-S_{\text{short}}}$ and the monopole operator associated to the root $\tilde{\alpha}$ at order $e^{-S_{\text{long}}}$, given as:

$$\begin{aligned} M_j &= e^{-\frac{8\pi^2}{g^2 N}} e^{2i\alpha_j \cdot \sigma} & 1 \leq j \leq N-1, \\ M_0 &= e^{-\frac{4\pi^2}{g^2 N}} e^{i\tilde{\alpha} \cdot \sigma}. \end{aligned} \quad (3.6)$$

This gives us the mass of the dual photons in terms of the coupling constant g^2 . In order to see how this mass depends on the circle size L , we define the strong scale Λ , by using the one-loop beta function:

$$(\Lambda L)^{\beta_0} = e^{-\frac{8\pi^2}{g^2}} = e^{-NS_{\text{short}}} = e^{-2NS_{\text{long}}}, \quad (3.7)$$

³We are only interested in theories with an even number of species in order to avoid the Witten anomaly [15]. However, we will derive our formulas for general n_f for overall consistency.

where $\beta_0 = \frac{11}{3}C_2(G) - \frac{2}{3}T(R)n_f$. With the aid of this definition, we derive the characteristic mass gap:

$$\begin{aligned} m_{\alpha_j \cdot \sigma} &\sim \frac{1}{L} e^{-\frac{S_{\text{short}}}{2}} = \Lambda(\Lambda L)^{\frac{\beta_0}{2N}-1} = \Lambda(\Lambda L)^{\frac{1}{6N}(5N+11-n_f)} \quad 1 \leq j \leq N-1, \\ m_{\tilde{\alpha} \cdot \sigma} &\sim \frac{1}{L} e^{-\frac{S_{\text{long}}}{2}} = \Lambda(\Lambda L)^{\frac{\beta_0}{4N}-1} = \Lambda(\Lambda L)^{\frac{1}{12N}(-N+11-n_f)}. \end{aligned} \quad (3.8)$$

For our approximation of the conformal window, we only look at the contribution of the short roots which provide the dominant contribution in the large N limit. We see that for fixed N and small n_f the generated mass grows as we increase L . As we increase n_f past the critical value $5N + 11$, the behavior flips and decreases with increasing circle size L . Therefore, according to the assertion in section 3, our estimate of the conformality bound is:

$$5N + 11 < n_f < 11(N + 1). \quad (3.9)$$

3.1.2 $SP(2N)$ with adjoint fermions

The case of the adjoint representation is similar among all simple Lie groups, with every monopole inheriting 2 zero modes from the instanton:

$$[I_0, I_1, \dots, I_N] = [2, 2, \dots, 2] \quad (3.10)$$

The mass gap is hence generated, to leading order, through composite objects called bions, which are comprised of one monopole M_j and an adjacent anti-monopole $M_{j\pm 1}$ [16]. The bions can be schematically depicted as links between the roots in the Dynkin diagram, figure 3.2. There are N such links, which would give mass to all N dual gauge fields:

$$B_j = M_j \overline{M_{j+1}} = \begin{cases} e^{-2S_{\text{short}}} e^{2i(\alpha_j - \alpha_{j+1}) \cdot \sigma} & 1 \leq j \leq N-2, \\ e^{-(S_{\text{short}} + S_{\text{long}})} e^{i(\tilde{\alpha} - 2\alpha_1) \cdot \sigma} & j = 0, \\ e^{-(S_{\text{short}} + S_{\text{long}})} e^{i(2\alpha_{N-1} - \alpha_N) \cdot \sigma} & j = N-1. \end{cases} \quad (3.11)$$

From this, one can read off the mass of the dual photons. Here, however, we note that at large N most of the fields become massive at order $\exp -2S_{\text{short}}$. Therefore, in this limit the generated mass gap for $N-2$ of the photons is:

$$m_\sigma \sim \frac{1}{L} e^{-S_{\text{short}}} = \Lambda(\Lambda L)^{\frac{\beta_0}{N}-1} = \Lambda(\Lambda L)^{\frac{1}{3N}(8N+11-2n_f(N+1))}, \quad (3.12)$$

where we have used (3.7) for the definition of the strong scale Λ . From this we obtain our estimate for the conformality bounds:

$$\frac{1}{2} \left(8 + \frac{3}{N+1} \right) < n_f < \frac{11}{2}. \quad (3.13)$$

3.1.3 $SP(2N)$ with 2-index anti-symmetric fermions

This representation can be considered as the compliment to the defining representation, in that it contains all the short roots whereas the defining representation contained all the long roots (with their length divided by 2). The index of the monopoles is given as:

$$[I_0, I_1, I_2, \dots, I_{N-1}, I_N] = [0, 2, 2, \dots, 2, 0]. \quad (3.14)$$

We see that the distribution of the zero modes is also the compliment of the defining representation where only the long root had a nonzero index. The mass gap is now generated through a combination of monopoles and bions:

$$\begin{aligned} M_j &= e^{-S_{\text{long}}} e^{i\alpha_j \cdot \sigma} & j = 0, N & \text{long roots,} \\ B_j &= M_j \overline{M_{j+1}} = e^{-2S_{\text{short}}} e^{2i(\alpha_j - \alpha_{j+1}) \cdot \sigma} & 1 \leq j \leq N-2 & \text{links between short roots.} \end{aligned} \quad (3.15)$$

In the large N limit, the predominant effect is that of the bions. Hence, the mass gap for all but 2 of the photons is:

$$m_\sigma \sim \frac{1}{L} e^{-S_{\text{short}}} = \Lambda (\Lambda L)^{\frac{\beta_0}{N}-1} = \Lambda (\Lambda L)^{\frac{1}{3N}(8N+11-2n_f(N-1))}, \quad (3.16)$$

where again we have used (3.7) to define Λ . The estimate for the conformality window is then:

$$\frac{1}{2} \left(8 + \frac{19}{N-1} \right) < n_f < \frac{11}{2} \frac{N+1}{N-1}. \quad (3.17)$$

3.2 Conformal windows for $SO(2N+1)$

The structure of the Lie group B_N or $SO(2N+1)$ is similar to that of C_N , as they share the same Coxeter graph. However, the different lengths of the roots makes the extended Dynkin diagram look very different. As can be seen from figure 3.3, the rank of the group is N , with 1 short root α_N and $N-1$ long roots. The extended root $\tilde{\alpha}$ is in this case a long root proportional to the fundamental weight λ_2 .

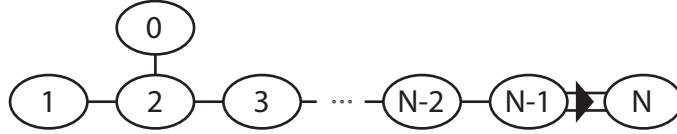


Figure 3.3: Extended Dynkin diagram of B_N . The root $\tilde{\alpha} = \alpha_0$ is proportional to λ_2 .

The structure of the vacuum is identical to the $SU(2N+1)$ case and is given by:

$$A_4|_\infty = \text{diag} \left(\frac{2N\pi}{2N+1}, \frac{2(N-1)\pi}{2N+1}, \dots, \frac{2\pi}{2N+1}, 0, -\frac{2\pi}{2N+1}, \dots, \frac{-2(N-1)\pi}{2N+1}, \frac{-2N\pi}{2N+1} \right). \quad (3.18)$$

Similar to the $SP(2N)$ case, a slight deformation of the effective potential is need to attain this structure in the case of the fundamental representation as well as the 2-index symmetric representation with $n_f = 1$. The same holds for $SO(2N)$. From this, we calculate the action of the monopoles:

$$\begin{aligned} S_{\text{long}} &= \frac{8\pi^2}{g^2(2N+1)} & \text{long roots,} \\ S_{\text{short}} &= S_{\tilde{\alpha}} = \frac{16\pi^2}{g^2(2N+1)} & \text{short roots and } \tilde{\alpha}. \end{aligned} \quad (3.19)$$

We will also use the strong scale derived from the one loop beta function:

$$(\Lambda L)^{\beta_0} = e^{-\frac{8\pi^2}{g^2}} = e^{-\frac{1}{2}(2N+1)S_{\text{short}}} = e^{-(2N+1)S_{\text{long}}}. \quad (3.20)$$

3.2.1 $SO(2N + 1)$ with fundamental fermions

The fundamental representation of $SO(2N + 1)$ is very similar to the 2-index antisymmetric representation of $SP(2N)$ discussed in section 3.1.3. Here, also, the representation is comprised of all the short roots. The index of the monopoles is hence:

$$[I_0, I_1, \dots, I_{N-1}, I_N] = [0, 0, \dots, 0, 2], \quad (3.21)$$

which implies that the monopoles associated to the long roots are responsible for generating a mass gap. Their explicit form is given as:

$$M_j = \begin{cases} e^{-\frac{8\pi^2}{g^2(2N+1)}} e^{i\alpha_j \cdot \sigma} & 1 \leq j \leq N-1, \\ e^{-\frac{16\pi^2}{g^2(2N+1)}} e^{i\tilde{\alpha} \cdot \sigma} & j = 0, \end{cases} \quad (3.22)$$

which are mostly at the scale $\exp -S_{\text{long}}$. The generated mass gap is then:

$$m_{\alpha_j \cdot \sigma} \sim \begin{cases} \frac{1}{L} e^{-\frac{1}{2}S_{\text{long}}} = \Lambda(\Lambda L)^{\frac{\beta_0}{2(2N+1)}-1} = \Lambda(\Lambda L)^{\frac{1}{6(2N+1)}(10N-17-2n_f)} & 1 \leq j \leq N-1, \\ \frac{1}{L} e^{-\frac{1}{2}S_{\tilde{\alpha}}} = \Lambda(\Lambda L)^{\frac{\beta_0}{(2N+1)}-1} = \Lambda(\Lambda L)^{\frac{1}{3(2N+1)}(16N-14-2n_f)} & j = 0, \end{cases} \quad (3.23)$$

where we have made use of the strong scale defined in equation (3.23). Taking only the predominant effect of the long roots into consideration, we derive our estimate of the conformality window:

$$\frac{1}{2}(10N - 17) < n_f < \frac{11}{2}(2N - 1). \quad (3.24)$$

3.2.2 $SO(2N + 1)$ with adjoint fermions

Similar to the adjoint representation of all other gauge groups, all the monopoles carry an equal number of zero modes. We have:

$$[I_0, I_1, \dots, I_N] = [2, 2, \dots, 2]. \quad (3.25)$$

Hence, the leading operators responsible for the mass gap are the bions. Again, the best way to visualize these operators is to think of them as the links between the roots of the extended Dynkin diagram (figure 3.3).

$$B_j = \begin{cases} M_j \overline{M}_{j+1} = e^{-2S_{\text{long}}} e^{i(\alpha_j - \alpha_{j+1}) \cdot \sigma} & 1 \leq j \leq N-2, \\ M_{N-1} \overline{M}_N = e^{-(S_{\text{short}} + S_{\text{long}})} e^{i(\alpha_{N-1} - 2\alpha_N) \cdot \sigma} & j = N-1, \\ M_0 \overline{M}_2 = e^{-(S_{\text{short}} + S_{\text{long}})} e^{i(\tilde{\alpha} - \alpha_2) \cdot \sigma} & j = 0. \end{cases} \quad (3.26)$$

Noting that the $N - 2$ of the photons receive mass at scale $\exp -S_{\text{long}}$, the estimate of the mass gap for large N is:

$$m_\sigma \sim \frac{1}{L} e^{-S_{\text{long}}} = \Lambda(\Lambda L)^{\frac{\beta_0}{2N+1}-1} = \Lambda(\Lambda L)^{\frac{1}{3N}(16N-14-2n_f(2N-1))}. \quad (3.27)$$

Where we have used equation 3.20. Which gives our estimate for the conformality window:

$$4 - \frac{3}{2N-1} < n_f < \frac{11}{2}. \quad (3.28)$$

3.2.3 $SO(2N + 1)$ with 2-index symmetric fermions

This representation of B_N is comprised of all the roots, as well as the weights which have twice the length of the short roots. This means that the index of the monopoles associated to the long roots is the same as the adjoint representation, while the index of the monopoles associated to the short roots and the root $\tilde{\alpha}$ is 3 times that of the adjoint representation:

$$[I_0, I_1, \dots, I_{N-1}, I_N] = [6, 2, \dots, 2, 6]. \quad (3.29)$$

The leading operators with zero magnetic charge and hence no zero modes are magnetic bions and quartets:

$$\begin{aligned} B_j &= M_j \overline{M_{j+1}} = e^{-2S_{\text{long}}} e^{i(\alpha_j - \alpha_{j+1}) \cdot \sigma} & 1 \leq j \leq N-2, \\ T_0 &= M_0 \overline{M_2^3} = e^{-(S_{\text{short}} + 3S_{\text{long}})} e^{i(\tilde{\alpha} - 3\alpha_2) \cdot \sigma}, \\ T_N &= M_{N-1}^3 \overline{M_N} = e^{-(S_{\text{short}} + 3S_{\text{long}})} e^{i(3\alpha_{N-1} - 2\alpha_N) \cdot \sigma}. \end{aligned} \quad (3.30)$$

Again, these composite operators can be visualized as the links between the roots on the extended Dynkin diagram. The operators B_j connect the α_j to α_{j+1} and the operators T_0 and T_N connect $\tilde{\alpha}$ to α_2 and α_{N-1} to α_N respectively.

This structure is more complex than the previous cases, however, we expect the magnetic bions to have the predominant effect at large N . Therefore, in this limit the generated mass gap would be:

$$m_\sigma \sim \frac{1}{L} e^{-S_{\text{long}}} = \Lambda (\Lambda L)^{\frac{\beta_0}{2N+1} - 1} = \Lambda (\Lambda L)^{\frac{1}{3N} (16N - 14 - 2n_f(2N+3))}. \quad (3.31)$$

The predicted range of conformality is then:

$$4 - \frac{19}{2N+3} < n_f < \frac{11}{2}. \quad (3.32)$$

3.3 Conformal windows for $SO(2N)$

The main differentiating feature of the Lie algebra D_N or $SO(2N)$ from the other classical Lie algebras is the branching of the Dynkin diagram on α_{N-2} (figure 3.4).

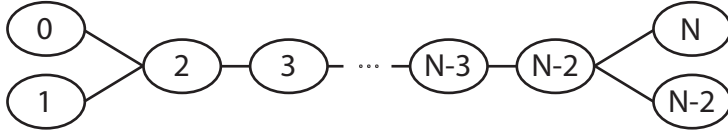


Figure 3.4: Extended Dynkin diagram of D_N . The root $\tilde{\alpha} = \alpha_0$ is proportional to λ_2 .

This means that there is, a priori, no specific order on the weights of the fundamental representation. Equivalently, one can say that elements of the Weyl group that fix the Weyl chamber, do not necessarily fix the vacuum of the theory. Here we make the choice:

$$w_{N+1}(A_4|_\infty) < 0 < w_N(A_4|_\infty), \quad (3.33)$$

which fixes the vacuum structure to:

$$A_4|_\infty = \text{diag} \left(\frac{(2N-1)\pi}{2N}, \frac{(2N-3)\pi}{2N}, \dots, \frac{\pi}{2N}, -\frac{\pi}{2N}, -\dots, -\frac{(2N-3)\pi}{2N}, -\frac{(2N-1)\pi}{2N} \right), \quad (3.34)$$

from which we calculate the action of the monopole operators:

$$S_i = \begin{cases} \frac{4\pi^2}{g^2 N} & 1 \leq j \leq N-1, \\ \frac{8\pi^2}{g^2 N} & j = 0, N. \end{cases} \quad (3.35)$$

The strong scale derived from the one loop beta function is:

$$(\Lambda L)^{\beta_0} = e^{-\frac{8\pi^2}{g^2}} = e^{-NS_0} = e^{-2NS_j} \quad 1 \leq j \leq N-1. \quad (3.36)$$

3.3.1 $SO(2N)$ with fundamental fermions

Similar to the other classical Lie algebras, the zero modes of the fundamental representation are localized to a single monopole. With equation (3.33) determining our base Δ , the only nonzero index is I_N :

$$[I_0, I_1, \dots, I_{N-1}, I_N] = [0, 0, \dots, 0, 2]. \quad (3.37)$$

Hence, the monopole operators are responsible for generating the mass gap. The mass of the dual photons is estimated at:

$$m_{\alpha_j \cdot \sigma} \sim \frac{1}{L} e^{-\frac{1}{2}S_j} = \begin{cases} \Lambda(\Lambda L)^{\frac{\beta_0}{4N}-1} = \Lambda(\Lambda L)^{\frac{1}{3}(10N-22-2n_f)} & 1 \leq j \leq N-1, \\ \Lambda(\Lambda L)^{\frac{\beta_0}{2N}-1} = \Lambda(\Lambda L)^{\frac{1}{3}(16N-22-2n_f)} & j = 0. \end{cases} \quad (3.38)$$

As before, we only consider the predominant effect in the calculation of the conformality window:

$$5N - 11 < n_f < \frac{11}{2}(2N - 2). \quad (3.39)$$

3.3.2 $SO(2N)$ with adjoint fermions

As previously mentioned, the zero mode distribution in the adjoint representation of all gauge groups is always equal across the board:

$$[I_0, I_1, \dots, I_N] = [2, 2, \dots, 2]. \quad (3.40)$$

With magnetic bions generating the mass gap to leading order. In this case the relevant operators are:

$$B_j = \begin{cases} M_j \overline{M_{j+1}} = e^{-2S_j} e^{i(\alpha_j - \alpha_{j+1}) \cdot \sigma} & 1 \leq j \leq N-2, \\ M_{N-2} \overline{M_N} = e^{-(S_{N-2} + S_N)} e^{i(\alpha_{N-2} - \alpha_N) \cdot \sigma} & j = N, \\ M_0 \overline{M_2} = e^{-(S_0 + S_2)} e^{i(\tilde{\alpha} - \alpha_2) \cdot \sigma} & j = 0. \end{cases} \quad (3.41)$$

Hence, our estimate of the mass gap for large N is:

$$m_\sigma \sim \Lambda(\Lambda L)^{\frac{\beta_0}{2N}-1} = \Lambda(\Lambda L)^{\frac{1}{3N}(16N-22-2n_f(2N-2))}. \quad (3.42)$$

Where we have used equation 3.36. The conformality bound is given by:

$$4 - \frac{3}{2N-2} < n_f < \frac{11}{2}. \quad (3.43)$$

3.3.3 $SO(2N)$ with 2-index symmetric fermions

With our choice of the base Δ (equation (3.33)), this case is almost identical to section 3.2.3. The representation is comprised of the roots plus twice the weights of the fundamental representation. The distribution of the zero modes is then:

$$[I_0, I_1, \dots, I_{N-1}, I_N] = [6, 2, \dots, 2, 6]. \quad (3.44)$$

The analysis is identical to section 3.2.3 with magnetic bions and quartets generating the mass gap:

$$\begin{aligned} B_j &= M_j \overline{M_{j+1}} = e^{-2S_j} e^{i(\alpha_j - \alpha_{j+1}) \cdot \sigma} & 1 \leq j \leq N-2, \\ T_0 &= M_0 \overline{M_2^3} = e^{-(S_0 + 3S_2)} e^{i(\tilde{\alpha} - 3\alpha_2) \cdot \sigma}, \\ T_N &= M_{N-1}^3 \overline{M_N} = e^{-(S_N + 3S_{N-1})} e^{i(3\alpha_{N-1} - 2\alpha_N) \cdot \sigma}. \end{aligned} \quad (3.45)$$

Again, these composite operators can be visualized as the links between the roots on the extended Dynkin diagram (figure 3.4). In the large N limit, we expect the magnetic bions to have the predominant effect, therefore, in this limit the generated mass gap would be:

$$m_\sigma \sim \Lambda(\Lambda L)^{\frac{\beta_0}{2N}-1} = \Lambda(\Lambda L)^{\frac{1}{3N}(16N-22-2n_f(2N+2))}. \quad (3.46)$$

The predicted range of conformality is:

$$4 - \frac{19}{2N+2} < n_f < \frac{11}{2}. \quad (3.47)$$

4. Comparison with other estimates of the conformal window

The results of section 3 are given in tables 4.1 to 4.6, for several values of N (referred to as Deformation Theory). Since the results for $SO(2N)$ and $SO(2N+1)$ are similar, they have been combined and appear in the table under $SO(N)$. For comparison we have also included the results from two other approaches: the ladder approximation using truncated Schwinger-Dyson equations, and the NSVZ-inspired approach with both $\gamma = 1$ and $\gamma = 2$ results (for a detailed review and derivation of these estimates see [17, 18, 19]). We also note that, for the cases at hand, there are no lattice results available that we are aware of.

We note that the comparison here bears a striking resemblance to a similar comparison carried out in [13] for the gauge group $SU(N)$. For all gauge groups the following holds. For the two indexed representations, the deformation theory approximation is close to the Schwinger-Dyson equation and is relatively far from the NSVZ-inspired estimates. However, for the the fundamental representation, the behavior flips and our approximation is much closer to the NSVZ-inspired estimate with $\gamma = 2$ and is far from the $\gamma = 1$ estimate and farther still from the Schwinger-Dyson numbers.

A comment on the peculiar results of $SO(N)$ with fundamental fermions (table 4.4) is in order. Unlike all our other results, for which the results for finite N as well as the asymptotic results match at least one of the other approaches, the results for finite N in this case don't come close to any of the other estimates. The reason behind this discrepancy is

our large N approximation. In the case of $SO(2N+1)$ ($SO(N)$ is similar), equation (3.23) tells us that for all but one of the photons the mass gap flips its behavior at $n_f = 5N - 8.5$. However for the one remaining photon the mass gap would flip its behavior at $n_f = 8N - 7$. This contribution should be ignored (as we do in our derivation) for large N , however, for small N one would expect the negligence of this term to result in the underestimation of the conformal bound, which is precisely what we see in our results in table 4.4.

N	Deformation Theory (monopoles)	Ladder (SD) approximation	NSVZ-inspired		Asymptotic Freedom bound
			$\gamma = 1$	$\gamma = 2$	
2	21	23.7	22	16.5	33
3	26	31.7	29.3	22	44
4	31	39.7	36.6	27.5	55
5	36	47.7	44	33	66
10	61	87.7	80.6	60.5	121
∞	$5N+11$	$8N+7.7$	$\frac{22}{3}(N+1)$	$\frac{11}{2}(N+1)$	$11(N+1)$

Table 4.1: Lower boundary estimate of the conformal window for $SP(2N)$ with fundamental fermions.

N	Deformation Theory (bions)	Ladder (SD) approximation	NSVZ-inspired		Asymptotic Freedom bound
			$\gamma = 1$	$\gamma = 2$	
2	4.5	4.15	3.67	2.75	5.5
3	4.37	4.15	3.67	2.75	5.5
4	4.3	4.15	3.67	2.75	5.5
5	4.25	4.15	3.67	2.75	5.5
10	4.13	4.15	3.67	2.75	5.5
∞	4	4.15	3.67	2.75	5.5

Table 4.2: Lower boundary estimate of the conformal window for $SP(2N)$ with adjoint fermions.

N	Deformation Theory (bions)	Ladder (SD) approximation	NSVZ-inspired		Asymptotic Freedom bound
			$\gamma = 1$	$\gamma = 2$	
2	13.5	12.2	11	8.25	16.5
3	8.75	8.18	7.33	5.5	11
4	7.16	7.17	6.11	4.58	9.17
5	6.375	6.37	5.5	4.12	8.25
10	5.05	5.05	4.48	3.36	6.72
∞	4	4.15	3.67	2.75	5.5

Table 4.3: Estimate of the lower boundary of the conformal window for $SP(2N)$ with 2-index anti-symmetric fermions.

N	Deformation Theory (monopoles)	Ladder (SD) approximation	NSVZ-inspired		Asymptotic Freedom bound
			$\gamma = 1$	$\gamma = 2$	
6	4	16.2	14.7	11	22
7	6.5	20.2	18.3	13.75	27.5
8	9	24.2	22	16.5	33
9	11.5	28.2	25.7	19.25	38.5
10	14	32.2	29.3	22	44
∞	$\frac{5}{2}N - 11$	$4N - 7.76$	$\frac{11}{3}(N - 2)$	$\frac{11}{4}(N - 2)$	$\frac{11}{2}(N - 2)$

Table 4.4: Lower boundary estimate of the conformal window for $SO(N)$ with fundamental fermions.

N	Deformation Theory (bions)	Ladder (SD) approximation	NSVZ-inspired		Asymptotic Freedom bound
			$\gamma = 1$	$\gamma = 2$	
6	3.25	4.15	3.67	2.75	5.5
7	3.4	4.15	3.67	2.75	5.5
8	3.5	4.15	3.67	2.75	5.5
9	3.57	4.15	3.67	2.75	5.5
10	3.62	4.15	3.67	2.75	5.5
∞	4	4.15	3.67	2.75	5.5

Table 4.5: Lower boundary estimate of the conformal window for $SO(N)$ with adjoint fermions.

N	Deformation Theory (bions)	Ladder (SD) approximation	NSVZ-inspired		Asymptotic Freedom bound
			$\gamma = 1$	$\gamma = 2$	
6	1.6	2.1	1.8	1.4	2.75
7	1.9	2.3	2.0	1.5	3.05
8	2.1	2.5	2.2	1.6	3.3
9	2.3	2.7	2.3	1.7	3.5
10	2.4	2.8	2.4	1.8	3.67
∞	4	4.15	3.67	2.75	5.5

Table 4.6: Estimate of the lower boundary of the conformal window for $SO(N)$ with 2-index symmetric fermions.

5. Conclusion

A quick look at the tables in section 4 as well as a comparison with the $SU(N)$ results from [13] shows that there are no surprises in our results: across the board the conformal bounds for all classical gauge groups are more or less the same, especially in the asymptotic limit. Of course, this was to be expected since for large N the classical gauge groups become virtually indistinguishable. Therefore, any hope of distinguishing the different cases rests in the finite N regime. However, the difficulty of deriving the coefficients of monopole and

composite monopole operators makes this calculation inaccessible. The same goes for the non-classical Lie groups.

Even though systematic improvements of our results are out of reach, with the aid of some heuristic arguments, it might still be possible to predict which class does the behavior of the mass gap of any given theory fall under (see figure 3.1). For example, equation (3.9) tells us that the conformality bound for fundamental fermions of $SP(2N)$ is $n_f^* \propto 5N$ in the large N limit and we know that perturbatively one adjoint fermion of $SP(2N)$ behaves like $2N$ fundamental fermions. We might, therefore, expect the conformality bound of the adjoint fermions of $SP(2N)$ to be $n_f^* \propto 2.5N$. The tension between this expectation and the actual result of $n_f^* \propto 4N$ from equation (3.13) implies that either the fundamental case is being underestimated or the adjoint calculation is an overestimate. Comparison with the results of other approaches seem to imply the former holds. Whichever the case is, we hope that in the future these arguments would help put our predictions in context.

Acknowledgments

We would like to thank E. Poppitz for continuous support throughout the project. We are also grateful to M. Ünsal for a generous amount of helpful comments.

APPENDIX

A. Lie Algebra Preliminaries

We follow the notation of [20]. Let G be a simple gauge group of rank l with \mathfrak{g} its Lie algebra. Denote \mathfrak{h} as the Cartan subalgebra, Φ as the set of all roots and w_i^R as the weights of a representation R . The weights correspond to maps $w_i^R : \mathfrak{h} \rightarrow \mathbb{R}$ and are hence elements of \mathfrak{h}^* . Weight spaces are defined as:

$$L_{w_i^R} = \{x \in R(\mathfrak{g}) \mid \forall h \in \mathfrak{h}, h(x) = w_i^R(h)x\}, \quad (\text{A.1})$$

and the roots are the weights of the adjoint representation. With this definition it is clear that by $w(h)$ we mean the eigenvalue of h corresponding to the weight w . For example if $h = \text{diag}(h_1, \dots, h_n)$ in the fundamental representation and w_i is the i 'th weight of the fundamental representation, we have $w_i(h) = h_i$.

We choose a basis for Φ such that all roots can be written as a sum over the basis elements with coefficients of the same sign. The elements of this basis are called simple roots and form the set Δ which is called a base.

Throughout this paper, we will use two properties of Lie algebras.

1. The existence of a non-degenerate bilinear form $b : \mathfrak{h} \times \mathfrak{h} \rightarrow \mathbb{R}$, $b(h_1, h_2) = \text{tr}(h_1 \cdot h_2)$ allows us to identify \mathfrak{h} with \mathfrak{h}^* : to $w \in \mathfrak{h}^*$ corresponds the unique element $t_w \in \mathfrak{h}$ satisfying:

$$w(h) = b(t_w, h) \quad \forall h \in \mathfrak{h}. \quad (\text{A.2})$$

The bilinear form b also defines⁴ an inner product on \mathfrak{h}^* given by:

$$w_1 \cdot w_2 = b(t_{w_1}, t_{w_2}) = w_2(t_{w_1}) = w_1(t_{w_2}). \quad (\text{A.3})$$

Using this inner product, we define the coroots as:

$$\alpha^* = \frac{2\alpha}{|\alpha^2|}, \quad (\text{A.4})$$

and the fundamental weights $\{\lambda_i\}$ as the members of the basis dual to the coroots:

$$\lambda_i \cdot \alpha_j^* = \delta_{ij}. \quad (\text{A.5})$$

2. If $\alpha \in \Phi$ and $x_\alpha \in L_\alpha$, $x_\alpha \neq 0$, then there exists $y_\alpha \in L_{-\alpha}$ such that $x_\alpha, y_\alpha, h_\alpha = [x_\alpha, y_\alpha]$ span a three dimensional simple subalgebra of L isomorphic to $\mathfrak{sl}(2, \mathbb{C})$ via:

$$x_\alpha \rightarrow \begin{pmatrix} 0 & 1 \\ 0 & 0 \end{pmatrix}, \quad y_\alpha \rightarrow \begin{pmatrix} 0 & 0 \\ 1 & 0 \end{pmatrix}, \quad h_\alpha \rightarrow \begin{pmatrix} 1 & 0 \\ 0 & -1 \end{pmatrix}. \quad (\text{A.6})$$

Here, the elements x_α and y_α are respectively the raising and lowering operators in the direction of the root α . Furthermore, we have:

$$h_\alpha = \frac{2t_\alpha}{b(t_\alpha, t_\alpha)} = \frac{2}{|\alpha|^2} t_\alpha = t_{\alpha^*}. \quad (\text{A.7})$$

In any root system, there is a unique root $\tilde{\alpha}$ such that:

$$y_\sigma(\tilde{\alpha}) = 0 \quad \forall \sigma \in \Delta, \quad (\text{A.8})$$

where y_σ is the lowering operator defined in property 2 above. The root $\tilde{\alpha}$ is called the lowest root (for obvious reasons). We define the extended base $\tilde{\Delta}$ as:

$$\tilde{\Delta} = \Delta \cup \{\tilde{\alpha}\}. \quad (\text{A.9})$$

It is conventional to pick out an orthogonal basis $\{T^a\}$ for the Cartan subalgebra:

$$b(T^a, T^b) = T(F)\delta^{ab}, \quad (\text{A.10})$$

where $T(F)$ is an arbitrary normalization. Using this basis we can expand any element of \mathfrak{h} as:

$$t = \frac{1}{T(F)} \sum_i b(t, T^a) T^a. \quad (\text{A.11})$$

⁴This is the only place our notation differs from [20] where the inner product is defined using the Killing form κ . The relation between the two definitions is given by

$$\kappa(t_1, t_2) = \frac{T(G)}{T(F)} b(t_1, t_2).$$

We can also use this basis to write any weight w as an l component vector $w^a = w(T^a)$. Using (A.3) we can write t_w , the corresponding element of \mathfrak{h} as:

$$t_w = \frac{1}{T(F)} \sum_a w^a T^a \equiv \frac{1}{T(F)} w \cdot H, \quad (\text{A.12})$$

and we have:

$$w \cdot v = b(t_w, t_v) = \frac{1}{T(F)} \sum_i w_i v_i. \quad (\text{A.13})$$

In this notation the length of the roots/weights as well as their inner products do not depend⁵ on the normalization $T(F)$.

For completeness, a summary of the Lie algebra data used in section 3 is given in table A.1.

Group	Algebra	Root lengths	Kac labels	Rep'n	$T(R)$
$SO(2N+1)$	B_N	$\{2, \dots, 2, 1\}$	$\{1, 2, \dots, 2, 1\}$	fund.	1
				sym.	$2N+3$
				adj.	$2N-1$
$SP(2N)$	C_N	$\{1, \dots, 1, 2\}$	$\{1, \dots, 1\}$	fund.	0.5
				anti-sym.	$N-1$
				adj.	$N+1$
$SO(2N)$	D_N	$\{2, \dots, 2\}$	$\{1, 2, \dots, 2, 1, 1\}$	fund.	1
				sym.	$2N+2$
				adj.	$2N-2$

Table A.1: Lie algebra data. The length of $\tilde{\alpha}$ is always 2 and its Kac label is 1 and is not included in the table.

References

- [1] B. Holdom, *Raising the Sideways Scale*, *Phys. Rev.* **D24** (1981) 1441.
- [2] K. Yamawaki, M. Bando, and K.-i. Matumoto, *Scale Invariant Technicolor Model and a Technidilaton*, *Phys. Rev. Lett.* **56** (1986) 1335.
- [3] T. W. Appelquist, D. Karabali, and L. C. R. Wijewardhana, *Chiral Hierarchies and the Flavor Changing Neutral Current Problem in Technicolor*, *Phys. Rev. Lett.* **57** (1986) 957.
- [4] M. A. Luty and T. Okui, *Conformal technicolor*, *JHEP* **09** (2006) 070, [[hep-ph/0409274](#)].
- [5] H. Georgi, *Unparticle Physics*, *Phys. Rev. Lett.* **98** (2007) 221601, [[hep-ph/0703260](#)].
- [6] E. Poppitz and M. Unsal, *Index theorem for topological excitations on $\mathbb{R}^3 \times S^1$ and Chern-Simons theory*, *JHEP.* **0903** (2009) 027, [[arXiv:0812.2085](#)].
- [7] C. Callias, *Index Theorems on Open Spaces*, *Commun. Math. Phys.* **62** (1978) 213–234.

⁵Equivalently, we can define the inner product as $w \cdot v = \sum_i w_i v_i$, in which case we would have to take $T(F) = 1$ to obtain the same results.

- [8] T. M. W. Nye and M. A. Singer, *An L^2 -Index Theorem for Dirac Operators on $S^1 \times \mathbb{R}^3$* , [math/0009144v1](#).
- [9] K.-M. Lee, *Instantons and magnetic monopoles on $\mathbb{R}^3 \times S^1$ with arbitrary simple gauge groups*, *Phys. Lett.* **B426** (1998) 323–328, [[hep-th/9802012](#)].
- [10] K.-M. Lee and P. Yi, *Monopoles and instantons on partially compactified D- branes*, *Phys. Rev.* **D56** (1997) 3711–3717, [[hep-th/9702107](#)].
- [11] E. J. Weinberg, *Fundamental monopoles and multimonopole solutions for arbitrary simple gauge groups*, *Nuclear Physics B* **167** (1980), no. 3 500 – 524.
- [12] N. M. Davies, T. J. Hollowood, and V. V. Khoze, *Monopoles, affine algebras and the gluino condensate*, *Journal of Mathematical Physics* **44** (2003) 3640.
- [13] E. Poppitz and M. Unsal, *Conformality or confinement: (ir)relevance of topological excitations*, *Journal of High Energy Physics* **2009** (2009), no. 09 050, [[arXiv:0906.5156](#)].
- [14] M. Shifman and M. Unsal, *QCD-like Theories on $R_3 \times S_1$: a Smooth Journey from Small to Large $r(S_1)$ with Double-Trace Deformations*, *Phys. Rev.* **D78** (2008) 065004, [[arXiv:0802.1232](#)].
- [15] E. Witten, *An $su(2)$ anomaly*, *Physics Letters B* **117** (1982), no. 5 324 – 328.
- [16] M. Unsal, *Magnetic bion condensation: A new mechanism of confinement and mass gap in four dimensions*, *Physical Review D (Particles, Fields, Gravitation, and Cosmology)* **80** (2009), no. 6 065001.
- [17] T. A. Ryttov and F. Sannino, *Supersymmetry inspired qcd beta function*, *Physical Review D* **78** (2008) 065001.
- [18] F. Sannino, *Conformal Windows of $SP(2N)$ and $SO(N)$ Gauge Theories*, *Phys. Rev.* **D79** (2009) 096007, [[arXiv:0902.3494](#)].
- [19] H. Pagels, *Departures from Chiral Symmetry: A Review*, *Phys. Rept.* **16** (1975) 219.
- [20] J. E. Humphreys, *Introduction to Lie Algebras and Representation Theory*. Springer, 1972.